Spatio-temporal multiplexing based on hexagonal multi-core fiber

I. CHEKHOVSKOY, M. SOROKINA, A. RUBENCHIK, M. FEDORUK, S. TURITSYN

August 30, 2017

Quantum Electronics

Disclaimer

Spatio-temporal multiplexing based on hexagonal multi-core fiber

I. S. Chekhovskoy[1,2,*], **M. A. Sorokina**[3], **A. M. Rubenchik**[4], **M. P. Fedoruk**[1,2], **and S. K. Turitsyn**[1,3]

[1] *Novosibirsk State University, Novosibirsk 630090, Russia*
[2] *Institute of Computational Technologies SB RAS, Novosibirsk 630090, Russia*
[3] *Aston Institute of Photonic Technologies, Aston University, Birmingham B4 7ET, UK*
[4] *Lawrence Livermore National Laboratory, Livermore, California 94550, USA*
[*] *Corresponding author: i.s.chekhovskoy@nsu.ru*

Compiled August 9, 2017

Recent progress in multi-core fiber technology offers new opportunities for spatio-temporal control of high-power light radiation. Here we apply the machine learning algorithms to design the system for a special type of nonlinear combining of high-power optical pulses based on hexagonal multi-core fiber. The pulses appear one by one in the consecutive cores of multi-core fiber schematically resembling operation of the revolver gun magazine.

OCIS codes: (190.4360) Nonlinear optics, devices; (060.4370) Nonlinear optics, fibers.

http://dx.doi.org/10.1364/ao.XX.XXXXXX

Switching of light between temporal and spatial domains have a range of applications from telecommunications to coherent pulse combining. For instance, in laser-based manufacturing and high-definition design of complex properties of materials, the surface of the treated metal product is exposed to a periodic sequence of high energy temporal optical pulses, where each pulse is focused onto certain spatial point in the product surface. Various schemes of linear beam/pulse combining are used to generate a high power optical beams [1]. An important requirement in coherent beam combining is the precise phase control of the input beams to maintain the output pulse coherence. The coherent beam combining is relatively simple for small arrays, however, combining of tens to hundreds of elements with high beam quality can be elusive.

Previously, using numerical simulations we have demonstrated the possibility of exploiting nonlinear effects in multi-core fibers (MCF) for the combining and compression of optical pulses [2, 3]. It was observed that in the MCF based approach, the requirements on the phase control can be weakened. Unlike conventional optical switch schemes [4], here we vary the input signal parameters, while the characteristics of the fiber remain fixed.

In this Letter, we demonstrate the design rules for a special type of nonlinear combining of high-power optical pulses at consequently selected core of MCF with two-dimensional arrangement of the cores, slightly resembling a pan magazine in the machine gun or revolver, in a sense that pulses appear one by one in the consecutive cores. The considered device makes multiplexing between temporal position of pulses into spatial domain. While it has been shown in previous studies the pulse combining in the central core [4], here we demonstrate using the machine learning approach how to effectively combine the optical pulses in any core by adjusting the parameters of the input pulses.

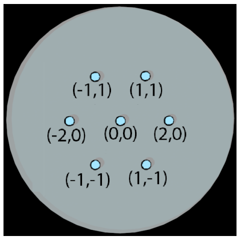

Fig. 1. Scheme of the considered 7-core hexagonal multi-core fiber.

Here without loss of generality we examine a 7-core hexagonal MCF (Figure 1). The discrete-continuous nonlinear Schrödinger equation (NLSE) was used for the numerical simulation of the optical pulse propagation along MCF and was solved by a generalization of the split-step Fourier method [5]. Gaussian pulses

$$U_{n,m}(z=0,t) = \sqrt{P_{n,m}} \exp\left[\frac{-(1+i\alpha_{n,m})t^2}{(2\tau_{n,m}^2)}\right] \exp\left(-i\phi_{n,m}\right), \quad \textbf{(1)}$$

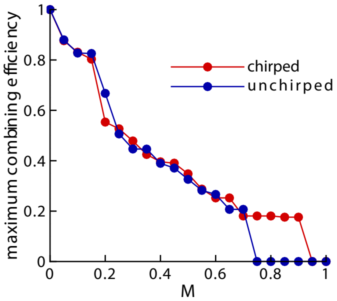

Fig. 2. Maximum combining efficiency of the pulse combined at peripheral core $(-2, 0)$ that can be obtained by amplitude modulation approach when amplitudes $P_{n,m}$ of input Gaussian pulses differ not more than M times. Red line denotes maximum efficiency when chirped initial pulses are used and blue line corresponds to the maximum efficiency of combining unchirped pulses.

where P is the amplitude, α is the chirp coefficient, τ denotes the pulse width, and ϕ is the phase shift. The considered model has a large number of optimization parameters calling for application of the machine learning approaches. Combining the machine learning algorithms with adaptive control it is potentially possible to develop self-tuning device. We apply here the standard genetic algorithm (GA), which is widely used in optics [6–12], for optimisation of the large number of parameters. We utilized the DEAP package [13] as a software implementation of GA written in Python and supporting parallel execution on the computing systems with distributed memory using SCOOP library [14]. In the GA the vector of input Gaussian pulse parameters (amplitudes, widths, phases and chirps) played role of a genotype of each individual in the population. Due to the problem symmetry for 7-core hexagonal MCF we can consider the parameters only of 5 pulses for each individual, thus reducing the size of the optimization problem. We will try to obtain combined pulse at the core $(-2, 0)$, so the pulse parameters for the cores $(-1, -1)$ and $(1, -1)$ equal the pulse parameters for the core $(-1, 1)$ and $(1, 1)$. The maximum pulse combining efficiency (the ratio of combined energy at the peripheral core to the total energy) that can be achieved by the pulses with specified parameters (genome) along the considered fiber was assigned as the value of the fitness function for each individual. Here it should be noted that the energy in the combined pulse «wings» was not taken into account in calculating the combining efficiency. We have considered two approaches to determining the Gaussian pulse parameters under which the combined pulse can be obtained in one of the peripheral cores of the 7-core hexagonal MCF.

The first approach is easier for practical realization (in the experiment) and it assumes that all pulses have equal parameters and only amplitudes differ. The initial phases of all Gaussian pulses are equal to zero. So the total number of parameters in the optimization problem to be solved (the genome size of a single individual in the genetic algorithm) is equal to 7. The genome values for the initial population are uniformly distributed random variables of the specified intervals. As mentioned earlier, the maximal combining efficiency of input Gaussian pulses obtained after calculating the propagation of these pulses along the MCF acted as the fitness function to evaluate the «quality» of individuals. Without any additional restrictions on the genomes of the individuals, it is necessary to inject the chirped pulse in the peripheral core with a peak power exceeding the peak power of all other pulses in several orders of magnitude in order to obtain the output pulse in this core, providing maximum combining efficiency. Of course, this solution is trivial and does not use nonlinear pulse combining. Therefore, we have introduced the restriction on the amplitude values of input Gaussian pulses:

$$\frac{\min P_{n,m}}{\max P_{n,m}} < M. \tag{2}$$

Using the GA we have found that if the amplitudes of the input pulses differ from each other by not more than 2 times, the maximal pulse combining efficiency that can be achieved is 34.8% (see figure 2). If the amplitudes do not differ by more than 5 times (figure 3), the maximal efficiency is equal to 55.3%. In this case the combined pulse was obtained at the distance along MCF $L = 0.57$ with the following initial Gaussian pulse parameters: $P_{-1,1} = 1.62321$, $P_{1,1} = 1.63567$, $P_{-2,0} = 7.90893$, $P_{0,0} = 2.62949$, $P_{2,0} = 1.82147$, $\phi_{n,m} = 0$, $\tau_{n,m} = 19.7325$, $\alpha_{n,m} = 37.8092$ $(\forall n, m)$. When the amplitude values differ in 10 times the maximal efficiency is about 83.1%. Moreover, we examine a necessary of including chirp parameter in the GA optimization: as one can see (figure 2), the parameter α can be neglected.

The second approach is more complicated from a technical point of view, since it requires a control of the initial phases of the input pulses. Here we set the pulses amplitudes, widths and chirps to be equal, but change the phase of each pulse individually, and thereby maximize the pulse combining efficiency in the peripheral core by adjusting 8 parameters. But the numerical simulation showed we can ignore the chirp parameter $\alpha_{n,m}$ – high combining efficiency can be obtained for unchirped pulses too. As a result, by using the GA the pulse parameters were

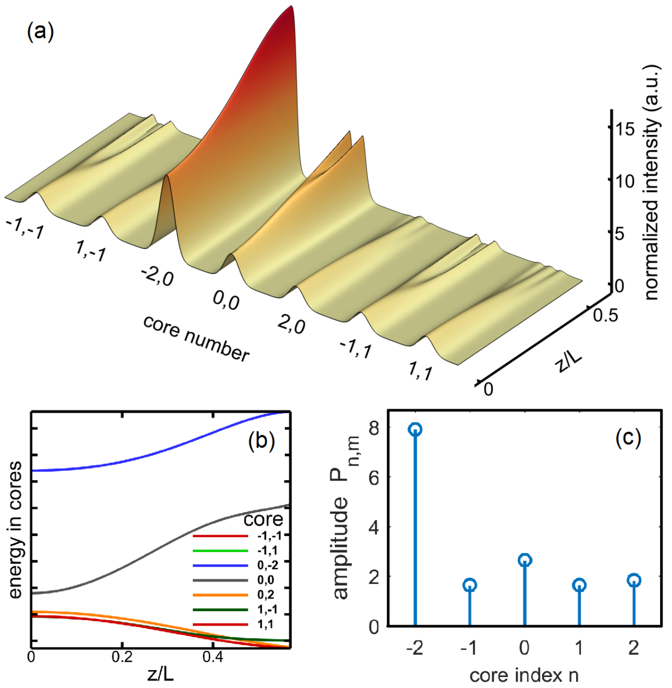

Fig. 3. The pulse intensity dynamics (a), the evolution of an energy by cores (b) for the solution obtained by the genetic algorithm using modulation of amplitudes ($M = 0.2$) with the maximum combining efficiency. The amplitudes $P_{n,m}$ of the input Gaussian pulses for various cores (c).

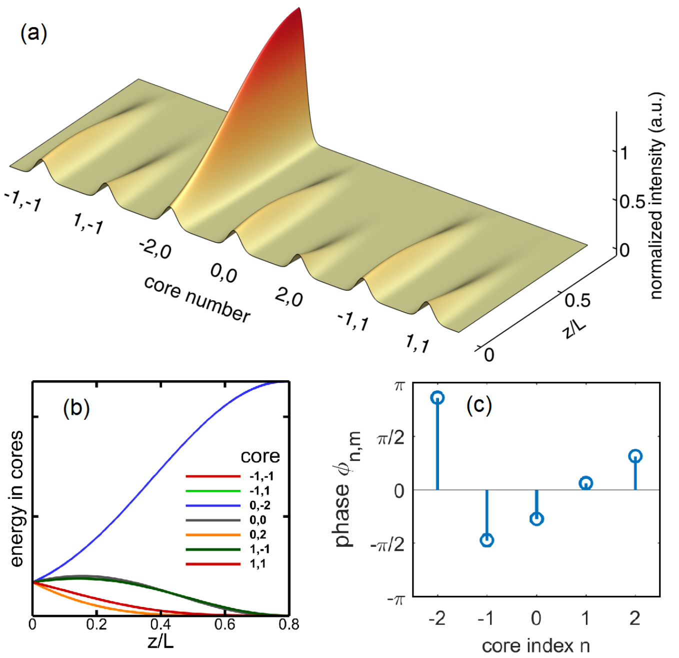

Fig. 4. The pulse intensity dynamics (a) and the evolution of an energy by cores (b) for the solution with combining efficiency about 99.4% obtained by the genetic algorithm using phase adjusting. The phases $\phi_{n,m}$ of the input Gaussian pulses for various cores (c).

obtained giving combining efficiency about 99.4% at the distance $L = 0.8$ (see (figure 4). The input Gaussian pulses in this case have parameters $P_{n,m} = 0.193203$, $\phi_{-1,1} = -1.49742$, $\phi_{1,1} = 0.183646$, $\phi_{-2,0} = 2.69176$, $\phi_{0,0} = -0.867763$, $\phi_{2,0} = 0.974319$, $\tau_{n,m} = 19.7550$, $\alpha_{n,m} = 0$.

The possibility of obtaining combined pulse at the equal distance along MCF both from peripheral and central cores is important condition for functioning of the proposed device. In the figure 5 the dependence of combining efficiency of the Gaussian pulses in the central core of 7-core hexagonal MCF and compression factor (the ratio of initial pulse width (FWHM) to the combined pulse width) for obtained pulses is presented (for details, please, see [3]). In these simulations equal Gaussian pulses with amplitudes P and width τ were introduced into all cores of the considered fiber. The white dashed line denotes regimes, when pulse combining occurs at the distance $z = 0.8$, as in the most effective regime within the phase selection approach. As one can see, at this distance in the central core the combining of 90% of the total energy can be achieved.

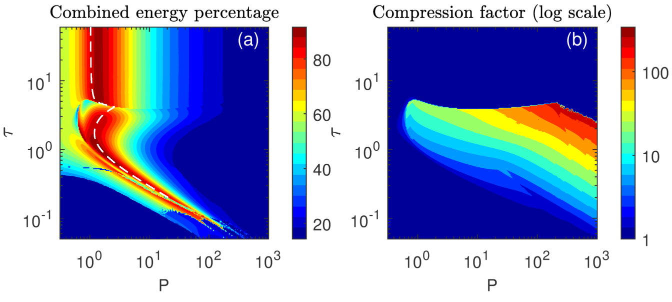

Fig. 5. The combining efficiency of the Gaussian pulses in the central core $(0, 0)$ and the compression factor for obtained pulses in the case of 7-core hexagonal fiber in dependence of the equal for all pulses amplitudes P and widths τ (see [3]). White dashed line corresponds to the pulses, which are combined at the distance $z = 0.8$, as in the regime presented in the figure 4.

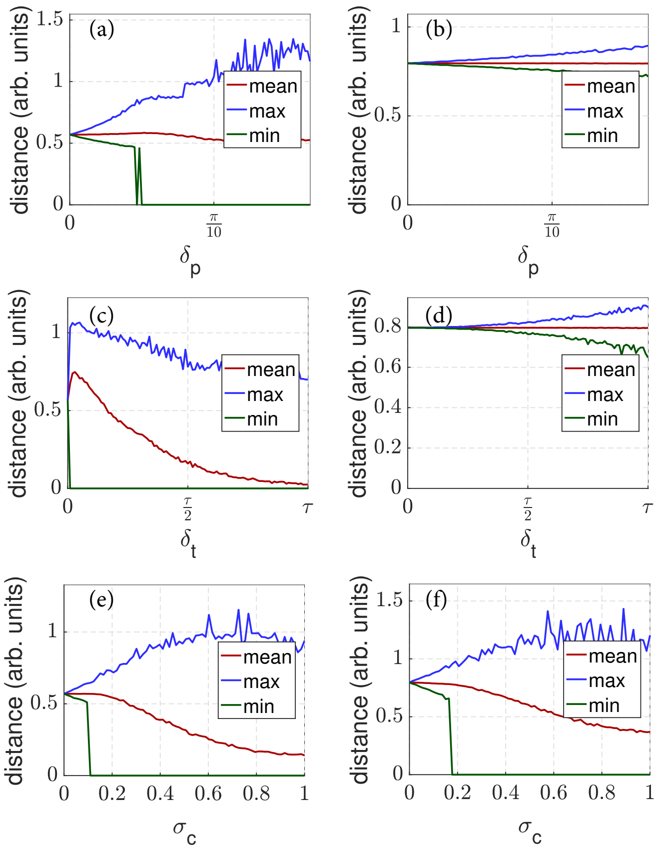

Fig. 6. The influence of phases mismatches (a,b), pulse delays (c,d) and coupling coefficient variance (e,f) on the distance to the combining point of the Gaussian pulses in the peripheral core $(-2, 0)$. Left figures correspond to the regimes with amplitude modulation ($M = 0.2$) and right figures refer to the regime with phase adjusting. The mean of the distance to the combining point was averaged over 2000 launches.

Numerical analysis of the impact of the fluctuations of initial pulse phases show that obtained regimes of both the first and second approaches have sufficient stability margin with respect to fluctuations of this type. However, first approach is sensitive to small temporal delays between the pulses. The results of a stability analysis for two regimes discussed earlier are presented in Figure 6. We consider the deviation of the combining distance, as one of the most important characteristic of combining scheme.

We modeled the phase perturbations as uniformly distributed on the segment $[-\delta_p; \delta_p]$ with a random function C_{δ_p}, so the initial pulses were

$$\tilde{U}_{n,m}(t) = U_{n,m}(t) \exp\left[-iC_{\delta_p}\right]. \qquad \textbf{(3)}$$

The parameter δ_p varied from 0 to π. All computed values were averaged over 2000 launches for every of 100 values of δ_p. The calculations showed that the combining scheme is stable for $\delta_p \in [0; \pi/20]$ in the case of the amplitude modulation regime and for $\delta_p \in [0; \pi/5]$. The distance to the combining point

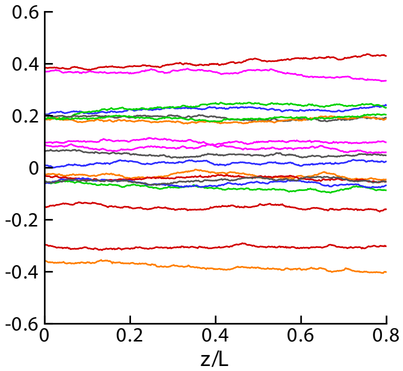

Fig. 7. An example of the realization of the random processes $\Delta C(z)$ for modeling the coupling coefficient fluctuations (standard deviation $\sigma_c = 0.1643$ for each z). Each process corresponds to one of the coupling coefficient.

along MCF (mean, maximum and minimum values) is shown in figure 6(a,b).

The random pulse delays were modeled as uniformly distributed on the segment $[-\delta_t; \delta_t]$ with the random function C_{δ_t}, making perturbed initial pulses

$$\tilde{U}_{n,m}(t) = U_{n,m}(t - C_{\delta_t}). \tag{4}$$

The simulations showed the stability of the combining scheme in the case of phase adjusting approach for $\delta_t \in [0; \tau]$, where $\tau = 19.755$ is the width of the injected pulses (see Fig. 6(d)). But the first approach is unstable with respect to fluctuations of this kind (Fig. 6(c)).

In the production of fibers, it is extremely important to preserve the geometry of the fiber cross-section over its entire length. However, the slight discharges of the distance between the cores, the core sizes, as well as the refractive index distribution are possible. All this ultimately affects the coupling coefficient C between the cores. So we have studied the effect of fluctuations in the coupling coefficient of a 7-core hexagonal fiber on the proposed combining schemes. These fluctuations were simulated using a Wiener random process $\Delta C(z)$, so the coupling coefficient represents in the following way:

$$C(z) = C_0 + \Delta C(z), \tag{5}$$

where C_0 is the mean value of the coupling coefficient ($C_0 = 1$ in current model). This approach allows relatively smooth change the value of the coupling coefficient along the fiber. Calculations showed that the proposed regimes are sufficiently sensitive to a variance in the coupling coefficient between the cores. The main characteristics begin to deteriorate significantly when the standard deviation of the coupling coefficients $\sigma_c(z)$ exceeds 10% for the regime with amplitude modulation and 15% for the regime with phase adjusting. However, such a requirement is feasible in practice: in the production of multi-core fibers, the distance between the cores fluctuates by an amount not exceeding 3–5%. The characteristic length of such deviations is about 10 meters. Thus, using a short enough (up to 10 meters) optical fiber, the proposed scheme will be resistant to possible inhomogeneities in the structure of the fiber.

This work was supported by the Russian Science Foundation (Grant No. 14-21-00110) (work of I.S.Ch. and M.P.F.) and by the European Office of Aerospace Research and Development (grant FA9550-14-1-0305) and the Grant of Ministry of Education and Science of the Russian Federation (agreement No. 14.B25.31.0003) (work of S.K.T.). The work was partially performed under the auspices of the U.S. Department of Energy by Lawrence Livermore National Laboratory under Contract DE-AC52-07NA27344 (work of A.M.R).

REFERENCES

1. M. Hanna, F. Guichard, Y. Zaouter, D. N. Papadopoulos, F. Druon, and P. Georges, Journal of Physics B: Atomic, Molecular and Optical Physics **49**, 062004 (2016).
2. A. M. Rubenchik, I. S. Chekhovskoy, M. P. Fedoruk, O. V. Shtyrina, and S. K. Turitsyn, Opt. Lett. **40**, 721 (2015).
3. I. S. Chekhovskoy, A. M. Rubenchik, O. V. Shtyrina, M. P. Fedoruk, and S. K. Turitsyn, Phys. Rev. A **94**, 043848 (2016).
4. J. Zhou, Opt. Express **23**, 22098 (2015).
5. I. Chekhovskoy, V. Paasonen, O. Shtyrina, and M. Fedoruk, Journal of Computational Physics **334**, 31 (2017).
6. E. Kerrinckx, L. Bigot, M. Douay, and Y. Quiquempois, Opt. Express **12**, 1990 (2004).
7. S. Rosen, D. Gilboa, O. Katz, and Y. Silberberg, arXiv preprint arXiv:1506.08586 (2015).
8. D. Askarov and J. M. Kahn, Journal of Lightwave Technology **33**, 4032 (2015).
9. J. P. da Silva, Microwave and Optical Technology Letters **55**, 281 (2013).
10. B. Ivorra, B. Mohammadi, P. Redont, L. Dumas, and O. Durand, International Journal of Computational Science and Engineering **2**, 170 (2006).
11. F. R. Arteaga-Sierra, C. Milián, I. Torres-Gómez, M. Torres-Cisneros, G. Moltó, and A. Ferrando, Opt. Express **22**, 23686 (2014).
12. L. Rosa and K. Saitoh, "Optimization of large-mode-area tapered-index multi-core fibers with high differential mode bending loss for ytterbium-doped fiber applications," in "36th European Conference and Exhibition on Optical Communication," (2010), pp. 1–3.
13. F.-A. Fortin, F.-M. De Rainville, M.-A. Gardner, M. Parizeau, and C. Gagné, Journal of Machine Learning Research **13**, 2171 (2012).
14. Y. Hold-Geoffroy, O. Gagnon, and M. Parizeau, "Once you SCOOP, no need to fork," in "Proceedings of the 2014 Annual Conference on Extreme Science and Engineering Discovery Environment," (2014), pp. 60:1–60:8.

FULL REFERENCES

1. M. Hanna, F. Guichard, Y. Zaouter, D. N. Papadopoulos, F. Druon, and P. Georges, “Coherent combination of ultrafast fiber amplifiers,” Journal of Physics B: Atomic, Molecular and Optical Physics **49**, 062004 (2016).
2. A. M. Rubenchik, I. S. Chekhovskoy, M. P. Fedoruk, O. V. Shtyrina, and S. K. Turitsyn, “Nonlinear pulse combining and pulse compression in multi-core fibers,” Opt. Lett. **40**, 721–724 (2015).
3. I. S. Chekhovskoy, A. M. Rubenchik, O. V. Shtyrina, M. P. Fedoruk, and S. K. Turitsyn, “Nonlinear combining and compression in multicore fibers,” Phys. Rev. A **94**, 043848 (2016).
4. J. Zhou, “Power splitting and switching in a multi-core fiber based on the multimode interference effect,” Opt. Express **23**, 22098–22107 (2015).
5. I. Chekhovskoy, V. Paasonen, O. Shtyrina, and M. Fedoruk, “Numerical approaches to simulation of multi-core fibers,” Journal of Computational Physics **334**, 31–44 (2017).
6. E. Kerrinckx, L. Bigot, M. Douay, and Y. Quiquempois, “Photonic crystal fiber design by means of a genetic algorithm,” Opt. Express **12**, 1990–1995 (2004).
7. S. Rosen, D. Gilboa, O. Katz, and Y. Silberberg, “Focusing and scanning through flexible multimode fibers without access to the distal end,” arXiv preprint arXiv:1506.08586 (2015).
8. D. Askarov and J. M. Kahn, “Long-period fiber gratings for mode coupling in mode-division-multiplexing systems,” Journal of Lightwave Technology **33**, 4032–4038 (2015).
9. J. P. da Silva, “Ge-doped microstrutured fiber design by genetic algorithm for directional coupling,” Microwave and Optical Technology Letters **55**, 281–285 (2013).
10. B. Ivorra, B. Mohammadi, P. Redont, L. Dumas, and O. Durand, “Semi-deterministic versus genetic algorithms for global optimisation of multichannel optical filters,” International Journal of Computational Science and Engineering **2**, 170–178 (2006).
11. F. R. Arteaga-Sierra, C. Milián, I. Torres-Gómez, M. Torres-Cisneros, G. Moltó, and A. Ferrando, “Supercontinuum optimization for dual-soliton based light sources using genetic algorithms in a grid platform,” Opt. Express **22**, 23686–23693 (2014).
12. L. Rosa and K. Saitoh, “Optimization of large-mode-area tapered-index multi-core fibers with high differential mode bending loss for ytterbium-doped fiber applications,” in “36th European Conference and Exhibition on Optical Communication,” (2010), pp. 1–3.
13. F.-A. Fortin, F.-M. De Rainville, M.-A. Gardner, M. Parizeau, and C. Gagné, “DEAP: Evolutionary algorithms made easy,” Journal of Machine Learning Research **13**, 2171–2175 (2012).
14. Y. Hold-Geoffroy, O. Gagnon, and M. Parizeau, “Once you SCOOP, no need to fork,” in “Proceedings of the 2014 Annual Conference on Extreme Science and Engineering Discovery Environment,” (2014), pp. 60:1–60:8.